Chemla Effect in Molten LiCl/KCl and LiF/KF Mixtures

Mauro C. C. Ribeiro*

Laboratório de Espectroscopia Molecular, Instituto de Química, Universidade de São Paulo, C.P. 26077, CEP 05513-970, São Paulo, SP, Brazil

Received: October 21, 2002; In Final Form: March 12, 2003

Molecular dynamics (MD) simulations of molten LiCl/KCl and LiF/KF mixtures at 1030 K and molar fraction $x = 0.5$ and also of pure components LiCl, KCl, LiF, and KF have been performed. The aim of the MD simulations was to calculate the internal mobilities of the Li^+ and the K^+ cations in order to reproduce the Chemla effect, that is, the strong composition dependence of the cations' internal mobilities. In line with experimental findings, it has been found by MD simulations that the isotherms of the internal mobilities of chlorides and fluorides belong to different patterns. Whereas the more usual pattern of isotherms found in the chloride mixture can be explained by simple structural and dynamical properties depending most on first-neighbor anion−cation pairs, these do not explain why a distinct pattern of isotherms is found in the fluoride mixture. Structure and structural relaxation in the simulated systems are further discussed by calculating partial static structure factors, $S_{\alpha\beta}(k)$, and intermediate scattering functions, $F_{\alpha\beta}(\mathbf{k}, t)$. Remarkable changes in the partial $S_{\mathrm{LiLi}}(k)$ are observed upon mixing; namely, an intermediate-range order develops in the mixtures as revealed by the presence of a pre-peak (or first sharp diffraction peak) at a wave vector k smaller than the main peak of $S_{\mathrm{LiLi}}(k)$. The intermediate-range order and an associated intermediate-range order dynamics are much more pronounced in LiF/KF than in LiCl/KCl, implying a strong coupling between the cations in LiF/KF. It is then proposed that structural and dynamical signatures for the different types of isotherms of internal mobilities in LiCl/KCl and LiF/KF are to be found in structural relaxation in a range beyond first-neighbor distances.

I. Introduction

Revealing the mechanism of ionic mobilities in molten salts is a fundamental issue applicable to the key role played by the conductivity of the melts in many of their industrial applications. Studying mixtures of two or more different salts is particularly interesting because many industrial processes actually use mixtures to decrease the melting temperature and also because one now has an additional variable, namely, the composition of the mixture, whose effect on the conductivity can be investigated easily. In the last four decades, extensive investigations of cation mobilities in mixtures of two salts with a common anion have been carried out.[1−3] The Chemla effect refers to the strong composition dependence of the internal mobilities of the cations, b_i, which is defined as the mobility of a given cation i in relation to the anions. The Chemla effect is the finding that the internal mobility of the large cation can be higher than the internal mobility of the small one at a low molar fraction of the latter.

Experimental isotherms of internal mobilities of cations in mixtures of two alkali salts with many different anions (e.g., halides, nitrates, carbonates, etc.) have been classified by Okada according to their patterns.[3] Hereafter labeling the small cation 1 and the large one 2 and expressing the composition in terms of the molar fraction of the latter, x_2, two basic patterns of isotherms are illustrated schematically in Figure 1. In type I, the internal mobility of 1 decreases upon mixing, whereas the internal mobility of 2 increases upon mixing. In type II, the mobilities of both the cations decrease upon mixing. Modifications on the basic patterns shown in Figure 1 lead to further classification as types I.a−e and types II.a and b.[3] The mobility of a given cation can be higher than the mobility of the other one in the whole concentration range so that the individual isotherms do not cross. This leads, for instance, to type I.c or type I.d according to $b_1 > b_2$ or $b_1 < b_2$, respectively, in the whole x_2 range. Even in a given mixture the slopes of the individual isotherms are very dependent on temperature so that the concentration at the crossing point changes with temperature.

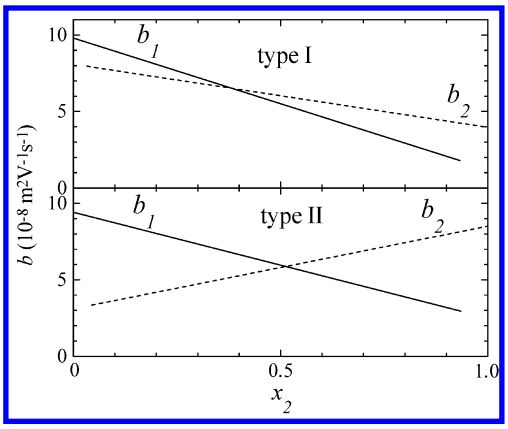

Figure 1. Schematic drawing of isotherms of internal mobilities of type I (top panel) and type II (bottom panel) in a molten salt M_1X/M_2X. The small cation is called cation 1, and the composition of the mixture is reported in terms of the molar fraction of the large cation, x_2. The solid lines correspond to the isotherms of b_1, and the dashed lines, to b_2.

* E-mail: mccribei@quim.iq.usp.br.

10.1021/jp027261a CCC: $25.00
Published on Web 04/15/2003

TABLE 1: Parameters of the Born−Mayer Potential Used in the MD Simulations[a]

	LiCl	LiCl/KCl[b]	KCl	LiF	LiF/KF[b]	KF
α	2.92	2.94	2.97	3.34	3.14	2.96
B_{--}	26544.9	28372.2	31104.1	6737.0	4164.3	2718.0
B_{-Li}	5202.3	5416.1		3669.0	2442.1	
B_{-K}		26424.4	28866.5		13544.8	8396.0
B_{LiLi}	798.7	821.2		1585.0	1136.3	
B_{LiK}		4352.5			7040.6	
B_{KK}		23072.2	25115.5		41301.7	24320.0
C_{--}	1110.0	1164.0	1245.0	145.0	162.9	186.0
D_{--}[c]	2230.0	2339.0	2500.0	0.0	0.0	0.0

C_{ClLi}	C_{FLi}	C_{ClK}	C_{FK}	C_{LiLi}	C_{LiK}	C_{KK}	D_{ClLi}[c]	D_{ClK}[c]	D_{LiLi}[c]	D_{LiK}[c]	D_{KK}[c]
20.0	8.0	480.0	195.0	0.73	13.3	243.0	24.0	730.0	0.3	8.5	240.0

[a] Units: α in Å^{-1}, B_{ij} in 10^{-20} J, C_{ij} in 10^{-20} J Å^6, and D_{ij} in 10^{-20} J Å^8. [b] Molar fraction $x = 0.5$. [c] In fluorides, all of the D_{ij} parameters were set equal to zero.

A full account of the observed patterns of the isotherms of internal mobilities can be found in recent reviews.[1−3] Isotherms of internal mobilities of type I are the more usual ones, to which the LiCl/KCl system belongs. It is explained by the strengthening of the small cation−anion association in an asymmetric environment experienced by the anion in such an arbitrary M_1^+−anion−M_2^+ arrangement. This picture has been corroborated by molecular dynamics (MD) simulations of alkali halide[4,5] and alkali nitrate[6] mixtures and by a neutron diffraction study of LiCl/CsCl.[7] These studies indicated enhancement and a shift to a smaller distance of the first peak of the partial cation 1−anion radial distribution function upon mixing. Thus, the Chemla effect is a nice example of the interplay between structure and dynamics because the tighter structure of a given cation 1−anion first-neighbor pair upon mixing correlates with the decrease in the internal mobility of small cation 1. Conversely, the cation 2−anion association is diminished upon mixing, which correlates with the increase in the internal mobility of large cation 2 as found in the isotherms of type I.

The isotherms of the internal mobilities of alkali chloride, bromide, and nitrate mixtures belong to the more usual type I.[3] However, LiF/KF is an example of the less usual type II because the internal mobility of both the Li^+ and K^+ cations decreases upon mixing. Why is the fluoride mixture such an exception? The purpose of this paper is to address this question by using MD simulations. It will be shown that the findings of the strengthening of the cation 1−anion association and the softening of the cation 2−anion association upon mixing, which nicely explain the isotherms of type I, are also found in the LiF/KF mixture. Therefore, one would not grasp the reason for the different pattern of isotherms in LiF/KF with the above argument, which relies only on first-neighbor cation−anion interactions.

The dynamics dissociation model[3,8] for the Chemla effect makes further assumptions to explain departures of the isotherms of internal mobilities from the usual pattern. For instance, a so-called tranquilizing effect is evoked in explaining the refrain of a dissociating step of a given cation−anion association and thus the reduction in its internal mobility due to the presence of other strongly interacting cations. The counterpart agitation effect is also proposed for some systems. These additional effects, which consider the role played by a second strongly interacting cation on the internal mobility of a given one, would correspond to the drag effect in the association model of Klemm.[9] These propositions lead us to the conclusion that structural or dynamical signatures for the differences in the isotherms of internal mobilities in LiCl/KCl and LiF/KF should be pursued in a range beyond first-neighbor distances.

It will be shown here that remarkable changes occur in the partial static structure factors, $S_{\alpha\beta}(k)$, upon mixing. The partial $S_{LiLi}(k)$ values in the mixtures display a peak at wave vector $k \approx 1.0$ Å, which is the so-called pre-peak or first sharp diffraction peak. The first sharp diffraction peak indicates an intermediate-range order because it appears in a k range that is smaller than k of the main peak. The first sharp diffraction peak as a signature of intermediate-range order is a well-known and intensely investigated issue mainly in the context of glass-forming liquids.[10] To my knowledge, this is the first time that it has been reported in molten alkali halide mixtures. Structural relaxation at different spatial ranges has then been studied by calculating the intermediate scattering function, $F_{\alpha\beta}(\mathbf{k}, t)$. It will be shown that the intermediate-range order and its corresponding intermediate-range order dynamics are more pronounced in the fluoride mixture than in the chloride mixture. This finding is correlated to the distinct types of isotherms of internal mobilities in LiCl/KCl and LiF/KF mixtures.

The paper is organized as follows. In section II, details of the MD simulations are given. In section III, the calculated internal mobilities and conductivities are reported. It is shown that the potential models used in the MD simulations are in fact able to give a composition dependence of the internal mobilities that corresponds to type I in the case of LiCl/KCl and type II in the case of LiF/KF. In section IV, several common structural and dynamical properties that are relevant in explaining the Chemla effect are reported for both the LiCl/KCl and the LiF/KF mixtures. The main conclusion of this section is that analogous findings are observed in both the LiCl/KCl and the LiF/KF systems so that one would not discern the reason for their different types of isotherms of internal mobilities. In section V, the structure and structural relaxation of the simulated systems are further discussed by means of $S_{\alpha\beta}(k)$ and $F_{\alpha\beta}(\mathbf{k}, t)$. Significant differences between LiCl/KCl and LiF/KF that would be helpful in understanding their different types of isotherms of internal mobilities are then discussed. Concluding remarks are given in section VI.

II. Computational Details

In this work, a pairwise additive Born−Mayer potential has been used in all of the MD simulations:[11]

$$V(\{\mathbf{r}\}) = \sum_{\substack{i,j \\ i<j}} \left[B_{ij} \exp(-\alpha r_{ij}) - \frac{C_{ij}}{r_{ij}^6} - \frac{D_{ij}}{r_{ij}^8} + \frac{q_i q_j}{r_{ij}} \right] \quad (1)$$

r_{ij} is the distance between ions i and j, and q_i is the charge of ion i. For completeness, all of the model parameters used in this work are given in Table 1. The well-known potential parameters α, B_{ij}, C_{ij}, and D_{ij} for the pure LiCl, KCl, LiF, and

KF melts have been used without changes.[11] In the case of the LiCl/KCl and LiF/KF mixtures, combining rules must be used for α, which is a single one in a given system $\alpha_{++} = \alpha_{--} = \alpha_{+-} = \alpha$, and also for the van der Waals coefficients between anions, C_{--} and D_{--}. The simple averaging rule proposed in previous simulations of NaCl/KCl[12] and LiCl/KCl[5] have also been applied in this work. The B_{ij} parameters in the mixtures are determined by the α parameters because B_{ij} (J) is given by $B_{ij} = (0.338 \times 10^{-19})\beta_{ij} \exp[\alpha(\sigma_i + \sigma_j)]$, with $\beta_{ij} = 1 + q_i/n_i + q_j/n_j$, where n_i is the number of electrons in the outer shells of ion i (eight for K^+, Cl^-, and F^- and two for Li^+), and σ_i is the ionic radii ($\sigma_{Li} = 0.816$ Å, $\sigma_K = 1.463$ Å, $\sigma_{Cl} = 1.585$ Å, and $\sigma_F = 1.179$ Å).[11] In the case of the MD simulations of the LiF/KF mixture, I have found close proximity between the Li^+ and the F^- species, which would lead to an eventual collapse between them as the van der Waals interactions become unphysically large at short distances. This problem with this kind of potential has also been observed in previous MD simulations of LiF at high pressures,[13] where the problem was circumvented by setting C_{+-} and D_{+-} equal to zero. In this work, the MD simulations of fluorides were performed with the D_{ij} parameters set equal to zero.

Experimental isotherms of internal mobilities for the LiCl/KCl mixture have been reported,[14] but unfortunately, the corresponding data for the LiF/KF mixture have not been reported. I stress that it will not be of concern here in drawing full isotherms of calculated internal mobilities and then in their further finer subdivision into types I.a−e and II.a and b.[3] Instead, the simulated systems have been chosen as representative examples in which b_1 decreases whereas b_2 increases upon dilution (the more usual type I, to which LiCl/KCl belongs) or in which both b_1 and b_2 decrease upon dilution (the less usual type II, to which LiF/KF belongs). Therefore, it is enough to compare the calculated internal mobilities in the pure components LiCl, KCl, LiF, and KF with the corresponding ones in the LiCl/KCl and LiF/KF mixtures at a single molar fraction, $x = 0.50$. All of the systems have been simulated at the same temperature (1030 K) to help with comparisons. The MD simulations considered 512 ions (256 anions and 256 cations) in an *NVE* ensemble in which the volume of the cubic simulation box corresponds to the experimental molar volume at 1030 K (LiCl, 29.51; KCl, 48.52; LiCl/KCl at $x = 0.50$, 39.01; LiF, 14.98; KF, 30.38; LiF/KF at $x = 0.50$, 22.66 cm^3/mol).[15,16] A Ewald sum was used to deal with the electrostatic interactions.[17] The time step in the MD simulations was 5.0 fs for the chlorides and 2.0 fs for the fluorides. Typical equilibration runs were 100.0 ps long, whereas typical production runs were 500.0 ps long.

Internal mobilities were calculated from the velocity collective time correlation functions[3,18]

$$C_{\alpha\beta}(t) = (N_-)\frac{1}{3}\left\langle \frac{1}{N_\alpha N_\beta} \sum_{i\in\alpha}\sum_{j\in\beta} \mathbf{v}_i(t)\cdot\mathbf{v}_j(0) \right\rangle \qquad (2)$$

where $\mathbf{v}_i(t)$ is the velocity of ion i at time t and N_α is the number of ions of species α (cation 1, cation 2, and − for the anions). The cation internal mobilities, b_1 and b_2, are calculated as the time integral of these time correlation functions:

$$b_{\alpha\beta} = \frac{e}{kT}\int_0^\infty K_{\alpha\beta}(t)\, dt \qquad (3)$$

e is the charge of the electron, k is the Boltzmann constant, T is the temperature, and $K_{\alpha\beta}(t)$ is a combination of the partial $C_{\alpha\beta}(t)$. The relevant $K_{\alpha\beta}(t)$ are[3,18]

$$K_{12}(t) = -C_{1-}(t) + C_{2-}(t) + x_1C_{11}(t) - x_2C_{22}(t) + (x_2 - x_1)C_{12}(t) \quad (4)$$

$$K_{+-}(t) = -2x_1C_{1-}(t) - 2x_2C_{2-}(t) + (x_1)^2C_{11}(t) + (x_2)^2C_{22}(t) + 2x_1x_2C_{12}(t) + C_{--}(t) \quad (5)$$

From the time integral of $K_{12}(t)$ and $K_{+-}(t)$, one obtains the corresponding b_{12} and b_{+-}, where $b_{+-} = x_1b_1 + x_2b_2$, which give the cation internal mobilities as[3,18]

$$b_1 = b_{+-} + x_2b_{12} \qquad (6)$$

$$b_2 = b_{+-} - x_1b_{12} \qquad (7)$$

Finally, the conductivity, κ, of the simulated system is given by $\kappa = (F/V)b_{+-}$, where F is the Faraday constant and V is the molar volume. In this work, the velocity collective correlation functions have been calculated as the average from two independent runs, each of them 500.0 ps long. The partial $C_{\alpha\beta}(t)$ were calculated up to 1.5 ps, which results in a good convergence in the time integral.

TABLE 2: Internal Mobilities (b_i in 10^{-8} m^2 V^{-1} s^{-1}), Conductivities (κ in S cm^{-1}), and Diffusion Coefficients (D_i in 10^{-5} cm^2 s^{-1}) Calculated by MD Simulations[a]

	b_{Li}	b_K	κ	D_-	D_{Li}	D_K	κ^{NE}	κ^{NE}/κ
LiCl	17.3 (19.1)[b]		5.7 (6.4)[c]	8.0	11.8		7.3	1.3
LiCl/KCl	9.6 (10.4)[b]	14.2 (12.7)[b]	2.9 (2.8)[c]	6.1	6.2	6.2	3.4	1.2
KCl		10.9 (10.7)[b]	2.2 (2.1)[c]	5.3		5.3	2.4	1.1
LiF	11.4		7.4 (8.4)[c]	6.6	7.6		10.4	1.4
LiF/KF	5.7	10.8	3.5 (3.0)[c]	6.3	5.0	5.0	5.5	1.6
KF		13.6	4.3 (3.4)[c]	6.9		5.1	4.4	1.0

[a] κ^{NE} is the conductivity estimated by the Nernst−Einstein equation (eq 9). Experimental values are given in parentheses. The errors in the calculated and experimental values are discussed in the text. [b] Extrapolated values by using empirical eq 8.[14] [c] Extrapolated values by using the empirical equations of refs 15 and 16.

III. Cation Internal Mobilities

Table 2 shows the cation internal mobilities, conductivities, and diffusion coefficients of the simulated systems. The calculated conductivities of chlorides are in good agreement with the experimental data.[15] In the case of fluorides, the agreement between calculated and experimental[16] conductivities is poorer but still satisfactory. (The uncertainty in the calculated κ and also in b_i is mainly due to the uncertainty in the convergence of the time integral due to noise in the velocity correlation functions at long time. This gives an estimated uncertainty of ± 0.3 S cm^{-1} in the calculated κ and not larger than 1.0×10^{-8} m^2 V^{-1} s^{-1} in the calculated b_i; typical uncertainties in the experimental data are 0.5% and $\pm 0.02 \times 10^{-8} m^2$ V^{-1} s^{-1}, respectively.[15,16]) It should be noted that, following the experimental results,[16] the calculated κ goes through a minimum in the LiF/KF mixture; that is, isotherms of κ are strongly nonideal in fluorides. In the LiCl/KCl mixture, κ also decreases nonideally upon diluting LiCl in KCl[15] but does not go through a minimum. The experimental b_{Li} and b_K given in Table 2 for chlorides are

extrapolated values obtained from the empirical relation between b_i, molar volume V_m, and temperature:[14]

$$b_i = \frac{A_i}{V_m - V_i} \exp\left(-\frac{E_i}{RT}\right) \quad (8)$$

R is the gas constant, and the parameters A_i, V_i, and E_i are $A_{Li} = 0.4858$ and $A_K = 6.080$ in 10^{-10} m^5 V^{-1} s^{-1} mol^{-1}, $E_{Li} = 26.62$ and $E_K = 38.86$ in kJ mol^{-1}, and $V_{Li} = 35.54-0.0169T$ and $V_K = 99.16-0.1079T$ in 10^{-6} m^3 mol^{-1}. Unfortunately, the experimental internal mobilities in fluorides have not been reported, but the calculated values in Table 2 seem reasonable in light of the results for chlorides and other binary alkali halide mixtures. Overall, the conductivities and internal mobilities shown in Table 2 suggest the adequacy of the potential models that have been used in the simulations.

The most important conclusion drawn from Table 2 is that b_{Li} decreases and b_K increases on going from pure melts LiCl and KCl, respectively, to the LiCl/KCl mixture. Thus, the isotherms of internal mobilities in LiCl/KCl belong to type I. However, in the LiF/KF mixture, both b_{Li} and b_K decrease on going from the corresponding pure melts to the mixture. Thus, the isotherms of internal mobilities in LiF/KF belong to type II. Therefore, the simulated systems indeed display the distinct patterns of the isotherms of internal mobilities as experimentally observed,[3] which is the main issue in this work.

Table 2 also shows the diffusion coefficients calculated from the slope at long time of the mean-square displacements, $\langle|\mathbf{r}_i(t) - \mathbf{r}_i(0)|^2\rangle = 6Dt$.[17] The calculated diffusion coefficients have been used in estimating the conductivities by the Nernst−Einstein equation:[19]

$$\kappa^{NE} = \frac{e^2}{kT}(\rho_- q_-^2 D_- + \rho_1 q_1^2 D_1 + \rho_2 q_2^2 D_2) \quad (9)$$

ρ_α is the number density of species α. The trend in D_{Li} and D_K mirrors the trend in b_{Li} and b_K upon mixing in both the LiCl/KCl and the LiF/KF systems, but the distinct nature of these properties should be noted as the reversal of internal mobilities in the equimolar mixtures because ($b_K > b_{Li}$) is not followed by the corresponding diffusion coefficients ($D_K = D_{Li}$). The departure of κ^{NE} from the actual κ indicates the relevance of cross correlation between the ions because the former is obtained from a single-particle time correlation function.[19] The largest κ^{NE}/κ ratio and also a clear drop of κ in the LiF/KF mixture lead us to the picture that the strongest interactions should be found in this system. In fact, these anion−cation associations and their effect on the isotherms of internal mobilities are the main subjects to be discussed in the following sections.

IV. Relating the Chemla Effect to Simple Structural and Dynamical Properties

One expects from any attempt to explain the Chemla effect some structural or dynamical signature for the observed composition dependence of the cation internal mobilities. A simple structural signature in the case of isotherms of internal mobilities of type I is found in the partial cation−anion radial distribution functions, $g_{\alpha\beta}(r)$. The argument is illustrated in Figure 2 for the LiCl/KCl system. It is clear that the first peak of $g_{ClLi}(r)$ is enhanced on going from pure melt LiCl to the LiCl/KCl mixture. The strengthening of the Cl^-−Li^+ association in the mixture is then responsible for the decrease in b_{Li} upon mixing. Conversely, the first peak of $g_{ClK}(r)$ is diminished on going from pure melt KCl to the LiCl/KCl mixture. The softening of the Cl^-−K^+ association in the mixture is then responsible for the increase in b_K upon mixing. This distinct behavior of the Cl^-−Li^+ and the Cl^-−K^+ associations upon dilution is also clear in the local order around each cation. As shown in the inset of Figure 2, the distribution of anions around a given K^+ undergoes a significant shift to larger coordination numbers upon dilution, whereas for Li^+ smaller coordination numbers are slightly more probable upon dilution.

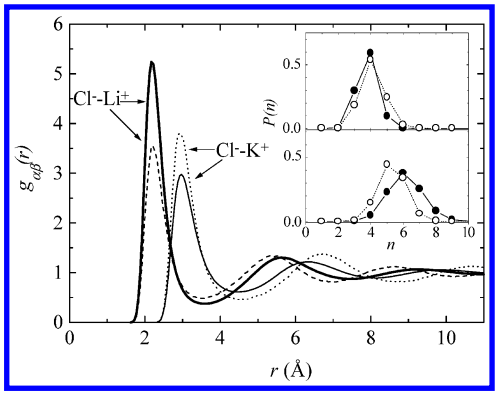

Figure 2. Anion−cation partial radial distribution functions, $g_{ClLi}(r)$ and $g_{ClK}(r)$, as indicated, calculated by MD simulations of pure LiCl, pure KCl, and the LiCl/KCl mixture at $x = 0.5$. The results for the mixture are shown as solid lines, and the results for the pure salts are shown as dashed lines. The inset shows the distribution of the number of first-neighbor anions around Li^+ (top panel in the inset) and K^+ (bottom panel in the inset). In the inset, the results for the pure melts are shown as white circles, and the results for the mixture are shown as black circles.

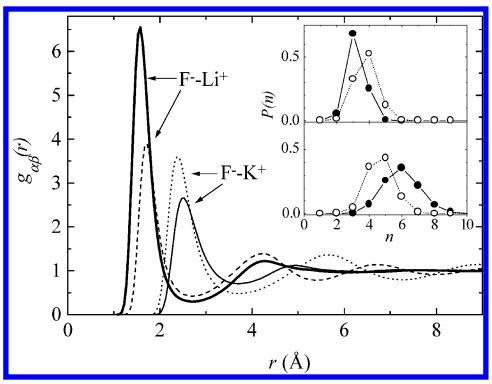

Figure 3. Same as Figure 2, but for the LiF/KF mixture.

The above finding is the starting point in proposed models for the Chemla effect, such as Klemm's association model[9] and Okada's dynamics dissociation model.[3,8] Thus, the explanation of the Chemla effect relies most on short-range, short-time associations and ruptures of anion−cation first-neighbor pairs. On this basis, the distinct pattern of isotherms of internal mobilities in the LiF/KF system should have a clear signature in the composition dependence of $g_{FLi}(r)$ and $g_{FK}(r)$. As Figure 3 shows, however, the overall changes in $g_{FLi}(r)$ and $g_{FK}(r)$ are similar to those in $g_{ClLi}(r)$ and $g_{ClK}(r)$ in the sense that the first peak of $g_{FLi}(r)$ is enhanced and the first peak of $g_{FK}(r)$ is diminished upon mixing. Were one to maintain the same argument that is used in explaining isotherms of type I, in the case of LiF/KF, the first peak of both $g_{FLi}(r)$ and $g_{FK}(r)$ should be enhanced to account for the decrease in both b_{Li} and b_K upon dilution in isotherms of type II. Because Figure 3 shows that this is not the case, one would expect from Figure 3 that the same consequence in LiCl/KCl would also follow in LiF/KF, that is, the decrease in b_{Li} and the increase in b_K upon dilution

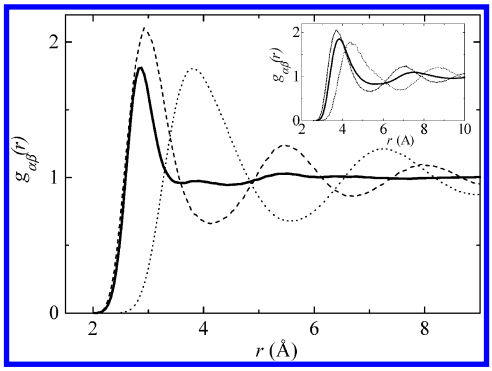

Figure 4. Anion−anion partial radial distribution functions, $g_{FF}(r)$, calculated by MD simulations of pure LiF (dashed line), pure KF (dotted line), and the LiF/KF mixture (solid line). The inset shows the corresponding $g_{ClCl}(r)$ for the LiCl/KCl mixture.

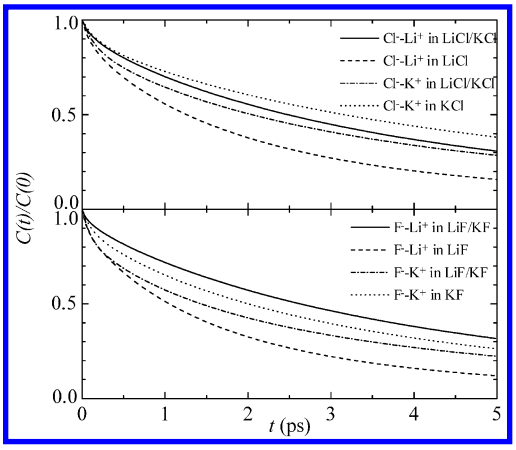

Figure 5. Correlation functions of residence times of first-neighbor anions around Li^+ and K^+. The top panel shows the results for the chlorides, and the bottom panel shows the results for the fluorides, as indicated.

(isotherms of type I). However, it has already been shown in the previous section that the isotherms in the LiF/KF system actually belong to type II, as experimentally observed. Therefore, the argument based on first-neighbor anion−cation associations is not enough to explain the distinct pattern of isotherms of internal mobilities in LiF/KF.

By comparing Figures 2 and 3, one notes that, although the overall trend in $g_{\alpha\beta}(r)$ is qualitatively similar in both the LiCl/KCl and LiF/KF mixtures, there is a clear difference in the magnitude of the observed mixing effects. The inset in Figure 3 shows that there is a remarkable change in the local order of anions around Li^+ in the LiF/KF mixture, in which the distribution becomes peaked on three-coordinated Li^+. Furthermore, the changes in $g_{FLi}(r)$ and $g_{FK}(r)$ are much more pronounced than in $g_{ClLi}(r)$ and $g_{ClK}(r)$. It is clear from Figure 3 that besides the enhancement of the first peak of $g_{FLi}(r)$ there is also a significant shift (∼0.13 Å) to smaller distances in the LiF/KF mixture in comparison with pure LiF. A shift of the first peak of $g_{FK}(r)$ to larger distances upon mixing is also evident in Figure 3. In addition, the oscillatory pattern in $g_{\alpha\beta}(r)$ is very much damped in the LiF/KF mixture. In fact, beyond the first peak, only the second peak is still discerned in $g_{\alpha\beta}(r)$ in LiF/KF, the third peak being almost completely smeared out. As shown in Figure 4, the finding that structural changes are much more pronounced in LiF/KF than in LiCl/KCl is made even clearer by comparing $g_{FF}(r)$ in the mixture to the corresponding ones in the pure components. The first peak of $g_{FF}(r)$ is shifted to smaller distances in LiF/KF in comparison with those in either LiF or KF, and the structure of $g_{FF}(r)$ beyond first-neighbor distances is very much washed out in the LiF/KF mixture. Overall, $g_{\alpha\beta}(r)$ reveals the large enhancement of local order upon mixing, which comes from the asymmetry of the potential experienced by an anion whose neighbors are disparate cations such as Li^+ and K^+. The distinct magnitude of the mixing effects on the structure of chlorides and fluorides is to be assigned to the small anion radii of the latter, which allows such close proximity between the species. Further consequences of the structural changes upon mixing and how they would help in understanding the distinct patterns of isotherms of internal mobilities in LiCl/KCl and in LiF/KF will be discussed in the next section.

The finding that arguments based on first-neighbor anion−cation associations do not explain the difference between the isotherms of internal mobilities of LiCl/KCl and LiF/KF should have an effect on dynamical signatures that have been proposed in addressing the Chemla effect. For instance, it has been shown by MD simulations that the internal mobility correlates with the so-called self-exchange velocity (SEV), which is defined by the time that a cation leaves the vicinity of a given anion.[3,20] (In fact, most of the MD simulation investigations of the Chemla effect have been devoted to the calculation of the SEV because it is calculated much more easily than the actual internal mobility.) In Figure 5, the dynamics of first-neighbor anion−cation pairs is investigated by means of time correlation functions of residence times, where such a pair is defined as long as the anion−cation distance is smaller than the first minimum of the corresponding $g_{\alpha\beta}(r)$ shown in Figures 2 and 3. The results for LiCl/KCl shown in the top panel of Figure 5 are in line with the composition dependence of the internal mobilities (isotherms of type I). The residence-time correlation function of Cl^- around Li^+ in the mixture decays slower than in pure LiCl, which is consistent with the decrease in b_{Li} upon mixing. Conversely, the residence-time correlation function of Cl^- around K^+ in the mixture decays faster than in pure KCl, which is consistent with the increase in b_K upon mixing. The results for LiF/KF shown in the bottom panel of Figure 5 display the same trend as LiCl/KCl so that again one would not discern why the isotherms of internal mobilities in LiF/KF belong to type II when the argument is based only on first-neighbor interactions.

Another commonly used dynamical signature of the nature of the Chemla effect is the composition dependence of the velocity correlation functions.[1,5] Figure 6 shows the single-particle velocity correlation functions of the cations in the simulated systems. It is clear that the well-known short-time rattling motion of Li^+ in temporary cages made by neighboring ions becomes more pronounced in the mixture. However, a lower frequency for such rattling motion is observed for K^+ in the mixture in comparison with that for the pure melts. These findings are similar in both the LiCl/KCl and LiF/KF systems. Whereas the results in Figure 6 are consistent with the decrease in b_{Li} and the increase in b_K in the mixture of chlorides, again they do not explain the decrease in both b_{Li} and b_K in the mixture of fluorides. Of course, the detailed shape of the single-particle velocity correlation functions shown in Figure 6 differs from the collective counterpart used in calculating b_i (not shown), but the above argument is the same.

In summary, common structural and dynamical properties that are relevant in explaining the Chemla effect have been discussed in this section. These results fully support the view proposed in previous models that are able to explain the pattern of isotherms of internal mobilities of type I, namely, that the composition dependence of internal mobilities is mainly deter-

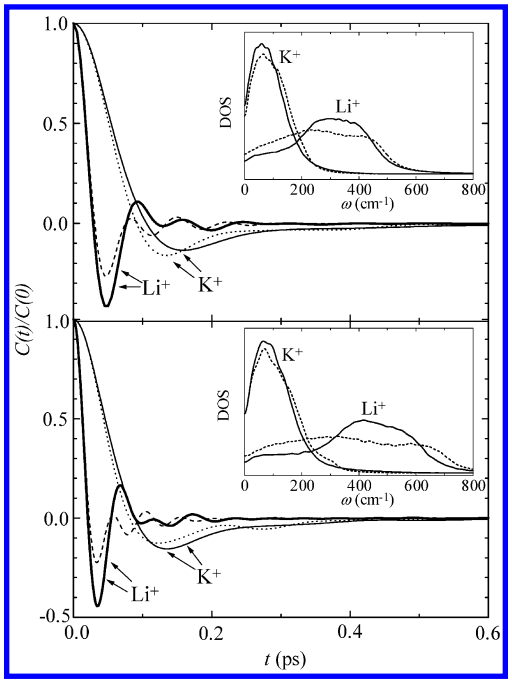

Figure 6. Normalized single-particle velocity correlation functions of Li^+ and K^+ as indicated. The top panel shows the results for the chlorides, and the bottom panel shows the results for the fluorides. The results for the mixtures are shown as solid lines, and the results for the pure salts are shown as dashed lines. The insets show the density of states (DOS) calculated by Fourier transforming the corresponding time correlation functions.

mined by structural and dynamical changes on first-neighbor anion−cation associations upon mixing.[1−3] However, from the properties shown, one would not grasp the reason for the isotherms of type II in fluorides because the composition dependence of these properties in fluorides is qualitatively similar to that in chlorides. It will be shown in the next section that a hint of the difference in their isotherms of internal mobilities can be found in the structure and structural relaxation in a range beyond first-neighbor distances.

V. Interpretating the Distinct Isotherms of Internal Mobilities in LiCl/KCl and LiF/KF

Proposed models for the Chemla effect would assign the decrease in b_K upon the dilution of KF in LiF, as observed in isotherms of type II, to some kind of coupling between the cations.[1−3] Although in a rather empirical and generic way, this proposition leads to a search of any structural signature of the difference between the isotherms of internal mobilities in LiCl/KCl and LiF/KF in a range beyond first-neighbor distances. The radial distribution functions $g_{\alpha\beta}(r)$ shown in Figures 2 to 4 indicated quantitative differences in how the local order changes upon mixing in these two systems. In discussing changes in next-neighbor shells, which would rely on discussing the small-amplitude oscillations of $g_{\alpha\beta}(r)$ at long range, it turns out to be more appropriate to use the static structure factor, $S_{\alpha\beta}(k)$. $S_{\alpha\beta}(k)$ is the spatial Fourier transform of the corresponding $g_{\alpha\beta}(r)$, but it has been calculated here directly from its definition to avoid numerical uncertainties:[19]

$$S_{\alpha\beta}(k) = \frac{1}{\sqrt{N_\alpha N_\beta}} \left\langle \sum_{i\in\alpha} \sum_{j\in\beta} e^{-i\mathbf{k}\cdot(\mathbf{r}_i - \mathbf{r}_j)} \right\rangle \qquad (10)$$

Figure 7 shows the calculated partial $S_{\alpha\beta}(k)$ of the LiF/KF mixture (solid lines) and the corresponding ones of pure melts LiF and KF (dashed lines). The change in $S_{LiLi}(k)$ upon the dilution of LiF in KF is remarkable. The intensity of the main peak decreases, and a new one at lower k appears in the mixture. This is the so-called pre-peak or first sharp diffraction peak, which implies that an intermediate-range order has developed in the liquid because it appears in a k range that is smaller than that of the main peak.

The first sharp diffraction peak as a signature of intermediate-range order has become a fundamental issue in the understanding of the structure and dynamics of glass-forming liquids.[10,21,22] It has been extensively studied by neutron-scattering spectroscopy and MD simulations of many different molecular and ionic glass-formers. To my knowledge, the presence of intermediate-

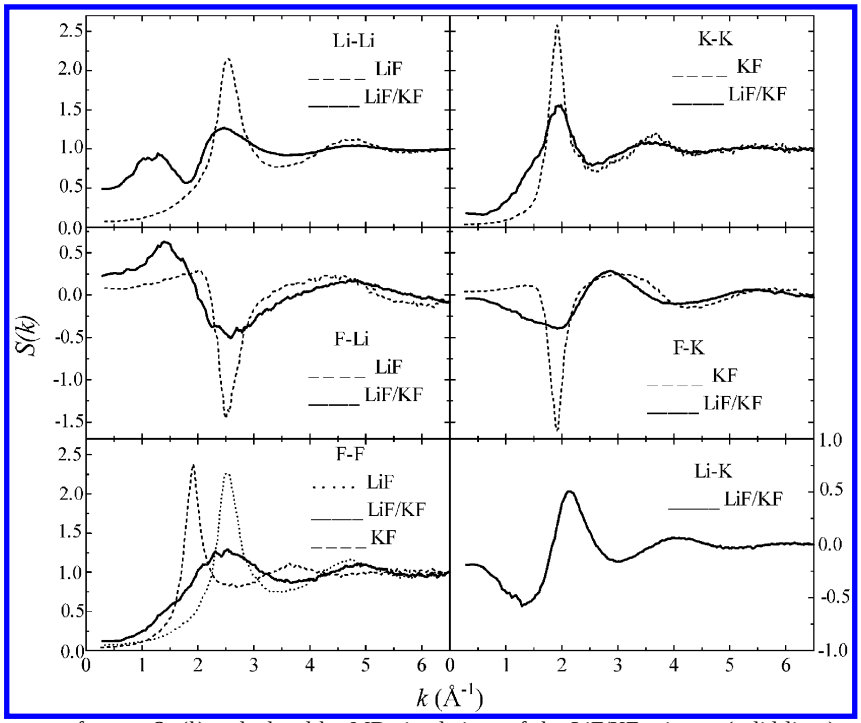

Figure 7. Partial static structure factors, $S_{\alpha\beta}(k)$, calculated by MD simulations of the LiF/KF mixture (solid lines) and pure melts LiF and KF (dashed lines).

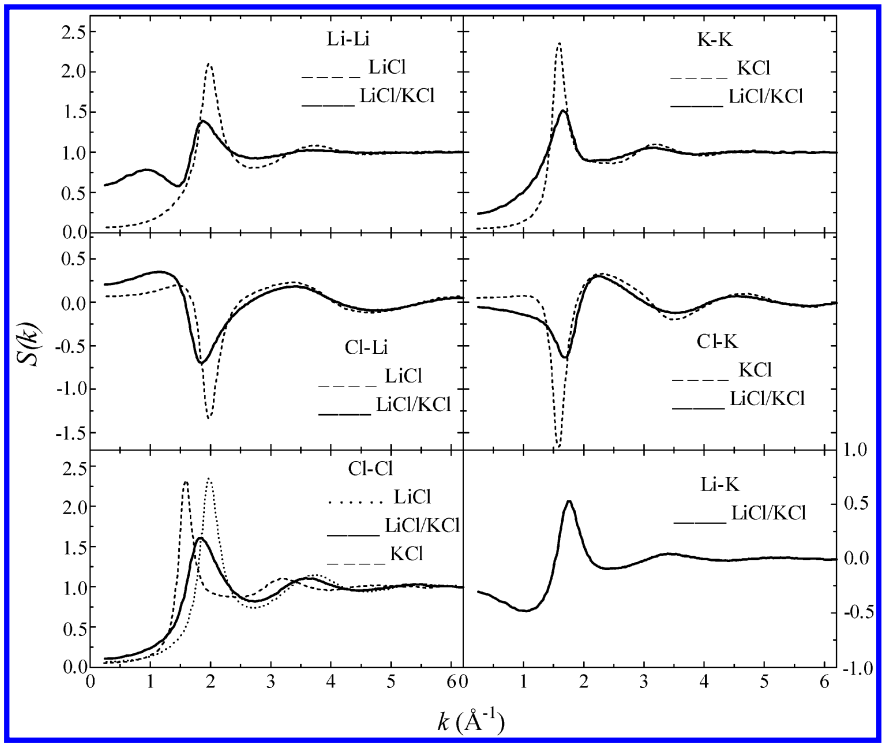

Figure 8. Same as Figure 7, but for the LiCl/KCl mixture.

range order in mixtures of two alkali halides has not been discussed before. The first sharp diffraction peak is not an exclusive feature of the LiF/KF system, as one can see in Figure 8, where the corresponding $S_{\alpha\beta}(k)$ values for the LiCl/KCl system are shown. However, there is a difference in the magnitude of the effect because the first sharp diffraction peak is much more pronounced in LiF/KF. It is clear that the intermediate-range order comes from the presence of two disparate cations such as Li^+ and K^+ because it would obviously disappear in the limit in which they are the same. In fact, in performing an additional MD simulation of NaCl/KCl with the potential parameters of ref 12, I have not observed the first sharp diffraction peak (not shown) that is characteristic of the presence of much more similar cations.

The nature of the intermediate-range order is still a matter of lively debate in the literature because different origins such as voids, layers, or clustering have been evoked, despite the similar phenomenology of the first sharp diffraction peak in many different molecular or ionic liquids.[23,24] In the case of several ionic systems, it is well known that the first sharp diffraction peak appears in the cations' partial $S_{\alpha\beta}(k)$ in MX_2 or MX_3 systems, for instance, the well-known glass-former $ZnCl_2$.[25] In these systems, it has been shown that modifications of the local structure are accompanied by an intermediate-range order. This new length scale comes from the voids generated in the melt due to nonuniformity in the spatial distribution of the cations. I propose that a similar effect is operating in the present case of alkali halide mixtures. As shown in Figure 9, distinct distributions of the Li^+ and K^+ cations in the simulation box can be identified by the direct visualization of an arbitrary configuration of the LiF/KF system. In the left panel of Figure 9, only the Li^+ ions are shown, whereas in the right panel only the K^+ ions of the same configuration are shown. In both the cases, first-neighbor ions have been connected, as long as the interionic distance is smaller than the first mininum of $g_{LiLi}(r)$ and $g_{KK}(r)$, respectively, 4.0 and 5.5 Å. In the case of the K^+ ions, it is clear that the connections between the ions fill up the simulation box in a homogeneous way. Conversely, the Li^+ ions

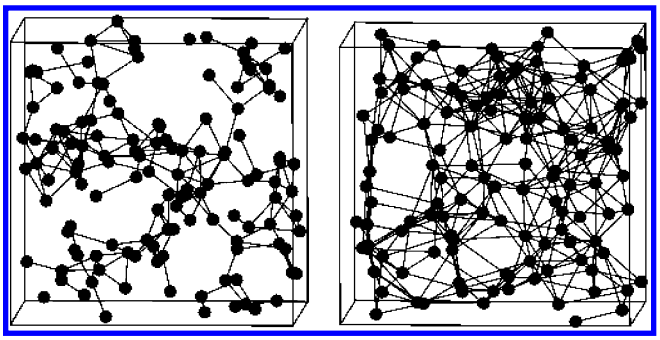

Figure 9. Snapshots of an arbitrary configuration obtained by MD simulation of the LiF/KF mixture. The left image shows only the Li^+ cations, and the right one shows only the K^+ cations of the same configuration. The lines connect the ions that are first neighbors as given by the position of the first minimum in $g_{LiLi}(r)$ and $g_{KK}(r)$, respectively, 4.0 and 5.5 Å.

distribute in a rather nonhomogeneous way, where voids can be identified in the Figure. Thus, a second, longer length scale develops in the mixture, giving rise to the first sharp diffraction peak in $S_{LiLi}(k)$. The effect is pronounced in fluorides and is characteristic of the small anionic radii that allow more significant changes in the local order, and therefore in the intermediate order, than in chlorides.

Further evidence of the distinct magnitude of the mixing effects on the structures of LiCl/KCl and LiF/KF is given in Figure 10, where the number density and charge structure factors, $S_{\rho\rho}(k)$ and $S_{qq}(k)$, respectively, are shown. These are properly weighted combinations of the partial $S_{\alpha\beta}(k)$ given by[19,26,27]

$$S_{\rho\rho}(k) = \sum_{\alpha\beta} (\rho_\alpha \rho_\beta)^{1/2} S_{\alpha\beta}(k) \tag{11}$$

$$S_{qq}(k) = \sum_{\alpha\beta} (\rho_\alpha \rho_\beta)^{1/2} q_\alpha q_\beta S_{\alpha\beta}(k) \tag{12}$$

The most significant observation related to Figure 10 is the substantial drop in the intensity of $S_{qq}(k)$ in LiF/KF. The major

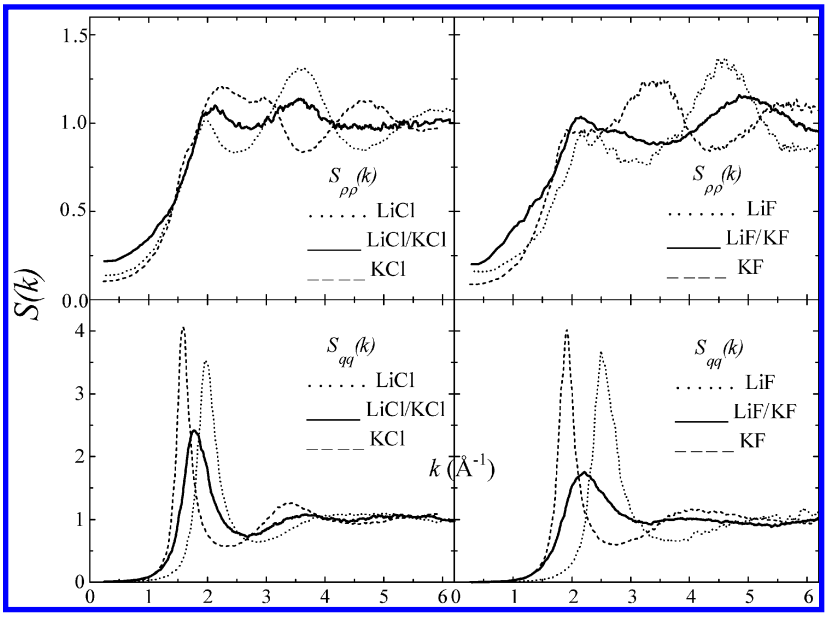

Figure 10. Number-density structure factor, $S_{\rho\rho}(k)$, and charge structure factor, $S_{qq}(k)$, calculated by MD simulations of chlorides and fluorides as indicated.

enhancement of local order in LiF/KF, as previously discussed also in real space by $g_{\alpha\beta}(r)$, results in a reduction of the simple charge-ordering effects. Proper to the weight factors in eqs 11 and 12, the contribution of the first sharp diffraction peak in $S_{\mathrm{LiLi}}(k)$ is diminished in Figure 10, although one can still discern a shoulder at $k \approx 1.2$ Å in $S_{\rho\rho}(k)$ in LiF/KF. Certainly any indication of the FSDP is absent in $S_{qq}(k)$ because its origin is not related to the charge fluctuations in ionic liquids.

Major structural changes upon mixing are revealed by the partial $S_{\mathrm{LiLi}}(k)$, but an inspection of Figures 7 and 8 indicates that they are also manifest in other partial $S_{\alpha\beta}(k)$ that are applicable to the coupled nature of the system. In case of LiF/KF (Figure 7), shoulders are observed in the range of the first sharp diffraction peak in $S_{\mathrm{KK}}(k)$, $S_{\mathrm{FK}}(k)$, and $S_{\mathrm{FF}}(k)$. In these partial $S_{\alpha\beta}(k)$, one notes that the main peak is broad and that it spreads over the range in which the first sharp diffraction peak appears in $S_{\mathrm{LiLi}}(k)$. Conversely, in LiCl/KCl (Figure 8), the low-k tail of the main peak in the corresponding $S_{\mathrm{KK}}(k)$, $S_{\mathrm{ClK}}(k)$, and $S_{\mathrm{ClCl}}(k)$ decays smoothly with no shoulders discernible. One expects that this evidence of the distinct magnitude of coupling in LiF/KF and LiCl/KCl on the equilibrium structure should be manifest in the corresponding dynamics.

To return to the main issue of this work, namely, the distinct pattern of the isotherms of internal mobilities in LiCl/KCl and LiF/KF, it is interesting to search for structural relaxation at some interesting wave vectors as dictated by these $S_{\alpha\beta}(k)$. Thus, partial intermediate scattering functions, $F_{\alpha\beta}(\mathbf{k}, t)$, have been calculated according to the expression[19]

$$F_{\alpha\beta}(\mathbf{k}, t) = \frac{1}{\sqrt{N_\alpha N_\beta}} \left\langle \sum_{i\in\alpha} \sum_{j\in\beta} \exp\{-i\mathbf{k}\cdot[\mathbf{r}_i(t) - \mathbf{r}_j(0)]\} \right\rangle \quad (13)$$

In fact, for a given k, $F_{\alpha\beta}(\mathbf{k}, t)$ has been calculated as an average of several different wave vectors $\mathbf{k}$ with the same modulus k. Among the six different partial $F_{\alpha\beta}(\mathbf{k}, t)$ available, the most interesting one, which is discussed in the following section, is the partial anion−cation $F_{\alpha\beta}(\mathbf{k}, t)$ because it reveals how the relaxation of the anion−cation structures at different spatial ranges changes upon mixing.

Partial $F_{\mathrm{ClLi}}(\mathbf{k}, t)$, $F_{\mathrm{FLi}}(\mathbf{k}, t)$, $F_{\mathrm{ClK}}(\mathbf{k}, t)$, and $F_{\mathrm{FK}}(\mathbf{k}, t)$ are shown in Figures 11−14, respectively. In each Figure, the top panel shows the results for the pure melt (LiCl, LiF, KCl, and KF, respectively), and the bottom panel shows the results for the mixture. The insets show the corresponding $S_{\alpha\beta}(k)$, in which the arrows indicate the wave vectors of the calculated $F_{\alpha\beta}(\mathbf{k}, t)$. The $F_{\alpha\beta}(\mathbf{k}, t)$ have been calculated at the smallest available wave vector ($k = 2\pi/L$, where L is the side of the simulation box), at the first sharp diffraction peak k_{FSDP}, at the main peak k_{m}, and at larger wave vectors. In these Figures, the $F_{\alpha\beta}(\mathbf{k}, t)$ were normalized by the one at k_{m}, that is, $F_{\alpha\beta}(k_{\mathrm{m}},0) = 1.0$, so that the relative intensities of the initial values of $F_{\alpha\beta}(\mathbf{k}, t)$ at different k's follow the intensity pattern of the corresponding $S_{\alpha\beta}(k)$ shown in the inset, except by the signal.

I first compare the relaxation of Li^+−anion structures in LiCl/KCl and LiF/KF (Figures 11 and 12). In the pure LiCl and LiF melts, as one expects, the most important contribution comes from relaxation at k_{m} that is characteristic of the significant structural order given by the strong peak in $S_{\alpha\beta}(k)$ at this wave vector. The relationship between the structure, structural relaxation, and internal mobilities, which has been calculated in real space in the previous section to explain the composition dependence of the internal mobilities, can be also calculated here in reciprocal space. For instance, by comparing $F_{\mathrm{ClLi}}(\mathbf{k}, t)$ at k_{m} in LiCl and LiCl/KCl (Figure 11), it decays more slowly in the latter, which correlates with the decrease in b_{Li} upon the dilution of LiCl in KCl. In a spatial range beyond the distance between next-neighbor shells given by k_{m}, that is, in the intermediate range given by the first sharp diffraction peak, relaxation at k_{FSDP} becomes very important in the mixtures. At this range, the different magnitude of the mixing effect in chlorides and fluorides is manifest. In comparison with the pure LiF melt, the structural relaxation of Li^+−F^- at an intermediate range becomes much more decisive in the LiF/KF mixture, and the effect is much more significant than the relaxation of the corresponding Li^+−Cl^- structures in LiCl/KCl. (Note the different scales in the bottom panels of Figures 11 and 12; in the latter, the initial value of $F_{\mathrm{FLi}}(\mathbf{k}, t)$ at k_{FSDP} is higher than at k_{m} because the $F_{\alpha\beta}(\mathbf{k}, t)$ were normalized by the one at k_{m}.) Thus, the new length scale of the intermediate-range order that develops upon mixing implies a corresponding intermediate-range order dynamics in the sense of slowing down density fluctuations in this spatial range. The comparison between

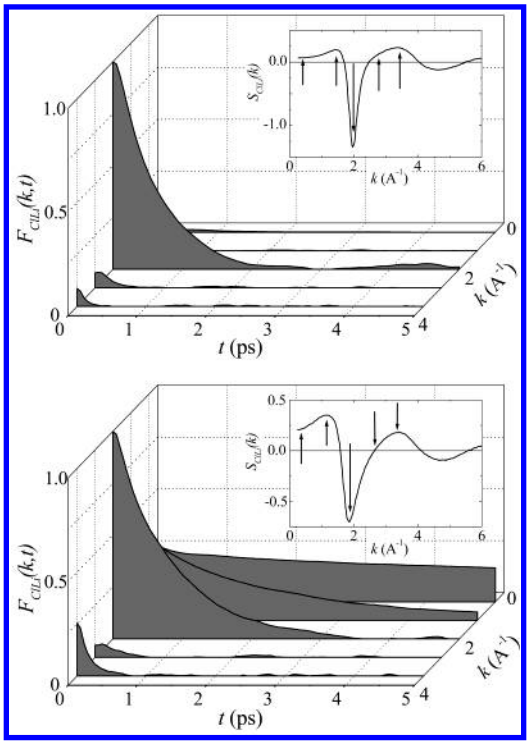

Figure 11. Cl^--Li^+ partial intermediate scattering functions, $F_{ClLi}(\mathbf{k}, t)$, calculated by MD simulations of pure LiCl (top panel) and the LiCl/KCl mixture (bottom panel). The insets show the corresponding static structure factor, $S_{ClLi}(k)$, where the arrows indicate the wave vectors of the calculated $F_{ClLi}(\mathbf{k}, t)$. The $F_{ClLi}(\mathbf{k}, t)$ have been normalized by the initial value of the corresponding one at k of the main peak in $S_{ClLi}(k)$.

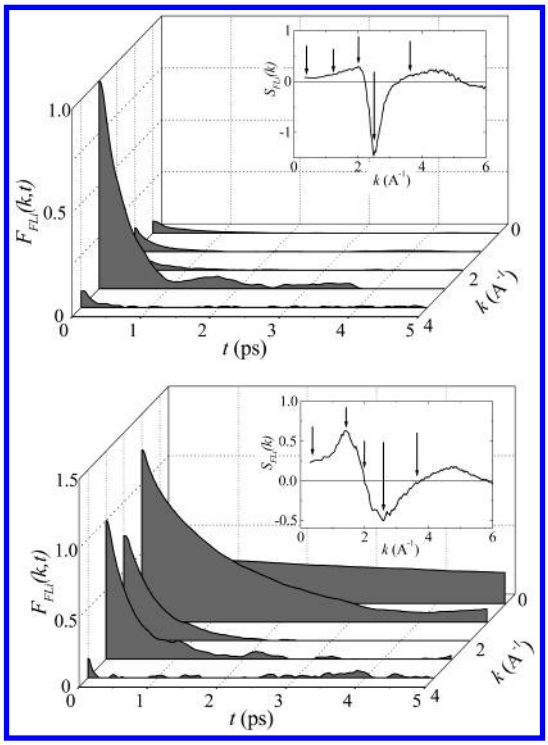

Figure 12. Same as Figure 11, but for the F^--Li^+ pair, $F_{FLi}(\mathbf{k}, t)$, for pure LiF (top panel) and the LiF/KF mixture (bottom panel). The insets show the corresponding static structure factor, $S_{FLi}(k)$.

Figures 11 and 12 indicates that this effect is dramatic in LiF/KF and less pronounced in LiCl/KCl.

I turn now to the discussion of the relaxation of K^+-anion structures in LiCl/KCl and LiF/KF (Figures 13 and 14). By comparing $F_{ClK}(\mathbf{k}, t)$ at k_m in KCl and LiCl/KCl (Figure 13), it

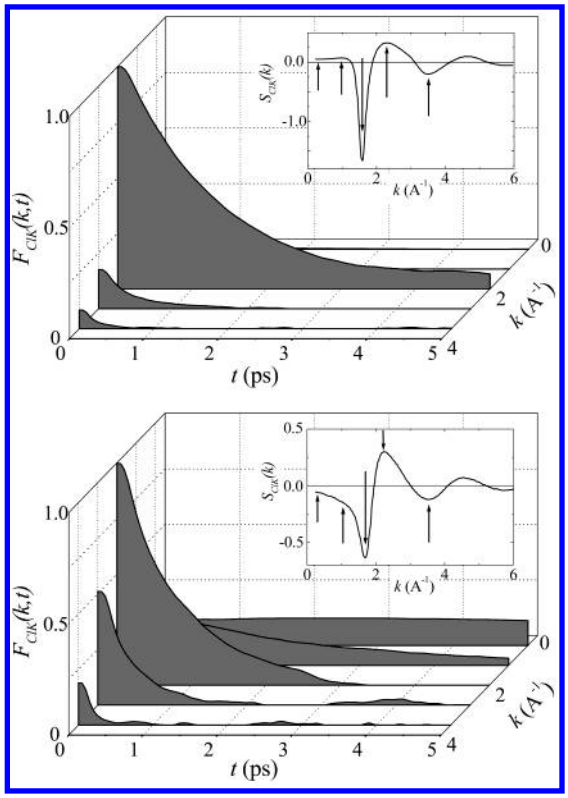

Figure 13. Same as Figure 11, but for the Cl^--K^+ pair, $F_{ClK}(\mathbf{k}, t)$, for pure KCl (top panel) and the LiCl/KCl mixture (bottom panel). The insets show the corresponding static structure factor, $S_{ClK}(k)$.

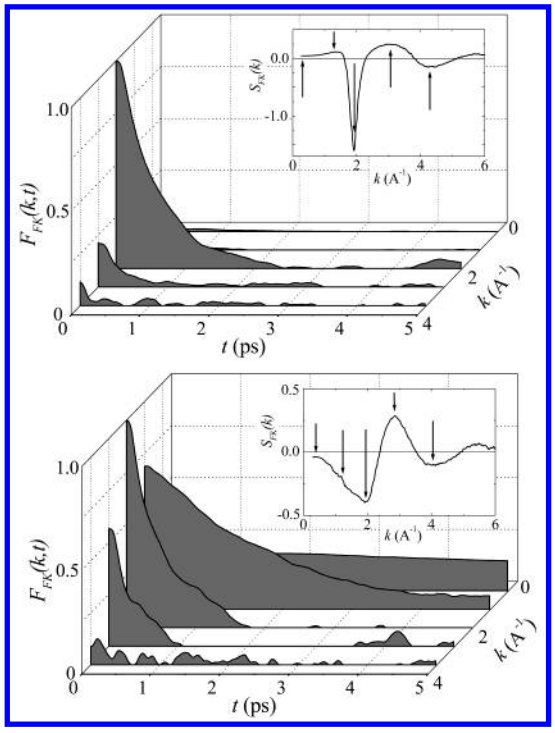

Figure 14. Same as Figure 11, but for the F^--K^+ pair, $F_{FK}(\mathbf{k}, t)$, for pure KF (top panel) and the LiF/KF mixture (bottom panel). The insets show the corresponding static structure factor, $S_{FK}(k)$.

is clear that it decays faster in the mixture, in contrast to the case of $F_{ClLi}(\mathbf{k}, t)$ shown in Figure 11. This correlates with the increase in b_K upon the dilution of KCl in LiCl, which together with the decrease in b_{Li} upon the dilution discussed above is the characteristic feature of isotherms of internal mobilities of type I. However, in the case of LiF/KF (Figure 14), the decay rate of $F_{FK}(\mathbf{k}, t)$ at k_m is similar in both the pure KF melt and

in the LiF/KF mixture. More remarkable is the difference between Figures 13 and 14 in the range of the first sharp diffraction peak. The structural relaxation of $F_{FK}(k_{FSDP}, t)$ is much more relevant in LiF/KF than the corresponding $F_{ClK}(k_{FSDP}, t)$ in LiCl/KCl. Therefore, this characteristic slow intermediate-range order dynamics given by $F_{FK}(\mathbf{k}, t)$ in the LiF/KF mixture implies the decrease in b_K on going from pure KF to LiF/KF, which, together with the fact that b_{Li} also decreases on going from LiF to LiF/KF, gives isotherms of internal mobilities of type II.

The above analysis of the relaxation of cation−anion structures at different spatial ranges and the possible relationship with cation internal mobilities lead us to the following picture. Short-range relaxation probed at k_m allows the interpretation of isotherms of internal mobilities of type I in very much the same line as the results in real space discussed in the previous section. In the case of LiCl/KCl, $F_{ClLi}(k_m, t)$ decays faster in pure LiCl than in the mixture, whereas $F_{ClK}(k_m, t)$ decays faster in the mixture than in pure KCl. This finding explains the decrease in b_{Li} and the increase in b_K on going from the pure melts to the mixture, that is, isotherms of type I. In the case of LiF/KF, b_{Li} also decreases on going from pure LiF to LiF/KF, which can be explained in the same line as in the chloride mixture. What remained to be explained is why, in contrast to the chloride mixture, b_K also decreases on going from pure KF to LiF/KF, that is, isotherms of type II. It has been found that $F_{FK}(k_m, t)$ decays almost at the same rate in both the pure KF melt and in the LiF/KF mixture. (Compare how $F_{ClK}(k_m, t)$ and $F_{FK}(k_m, t)$ in Figures 13 and 14, respectively, change on going from the pure melt to the mixture.) However, the most remarkable difference between the chloride and the fluoride mixtures is found at an intermediate range probed by k_{FSDP}. At this intermediate range, the slow relaxation of $F_{FK}(k_{FSDP}, t)$ is a significant contribution, but not in the chloride counterpart. This finding is then a hint for the decrease in b_K on going from pure KF to LiF/KF, as in isotherms of internal mobilities of type II. It should be noted that the characteristic intermediate-range order in both the chloride and the fluoride mixtures is being promoted by the Li^+ cations because the first sharp diffraction peak is mainly observed in the partial $S_{LiLi}(k)$. However, the difference in the magnitude of this mixing effect between these two systems, which is to be assigned to the small radii of the fluoride anion, gives rise in LiF/KF to the incipient first sharp diffraction peaks observed only as shoulders in other partial $S_{\alpha\beta}(k)$ including the K^+ species. This implies that the characteristic relaxation of K^+-F^- structures at intermediate range is playing a role in the LiF/KF mixture. In other words, there is a strong structural and dynamical coupling between the two cations in the LiF/KF mixture so that both b_{Li} and b_K decrease when the respective pure melts LiF and KF are mixed with each other (isotherms of type II).

VI. Concluding Remarks

The Chemla effect in LiCl/KCl and LiF/KF has been investigated by using MD simulations. It has been shown that the usual potential models for these systems are able to give the observed composition dependence of the cation internal mobilities b_i. Most significant is the finding that the calculated internal mobilities actually display the distinct pattern of isotherms as observed experimentally. In LiCl/KCl, b_{Li} decreases, and b_K increases as the corresponding pure melts LiCl and KCl are diluted in each other. These kinds of isotherms of internal mobilities are called isotherms of type I. In LiF/KF, both b_{Li} and b_K decrease upon mixing, which characterizes the isotherms of type II. Isotherms of type I are more common and are easily explained in terms of anion−cation first-neighbor structures and dynamics. By a simple inspection of the partial radial distribution functions $g_{\alpha\beta}(r)$, one sees that short-range Li^+-Cl^- structures are strengthening in the LiCl/KCl mixture, whereas K^+-Cl^- structures are softening, in comparison to the situation in the pure melts. This implies the decrease in b_{Li} and the increase in b_K upon mixing. Although this is a quite satisfactory explanation in the case of isotherms of type I, it does not help in understanding the distinct pattern of isotherms of type II in LiF/KF. In this case, b_K also decreases, as b_{Li} does, upon mixing LiF and KF. However, the mixing effects on $g_{\alpha\beta}(r)$ in LiF/KF are qualitatively similar to those in LiCl/KCl so that one would expect the same type of isotherms (type I) in both systems.

An inspection of $g_{\alpha\beta}(r)$ revealed a difference in the magnitude of the mixing effects between LiCl/KCl and LiF/KF. The changes in local order on mixing is much more dramatic in LiF/KF than in LiCl/KCl. This is simply assigned as a consequence of the small radius of the fluoride anion, which allows ions in the mixture to be in close proximity to one another. At this point, proposed models for the Chemla effect take into account additional effects that could be responsible for some kind of coupling or drag effects between the cation mobilities.[1−3] This proposition is reinforced by the fact that unusual decreases in mobilities are commonly seen when the system includes strongly interacting species, such as divalent cations. For instance, the tranquilizing effect proposed in the dissociation dynamics model occurs when a given strongly interacting cation makes it difficult for the other cation to leave the neighborhood of an anion. This kind of proposition leads one to think about structural and dynamical couplings that extend beyond typical first-neighbor distances. What I have done in this work is to search for a microscopic characterization of these proposed couplings.

To investigate longer-range structural relaxation in the simulated systems, I worked in reciprocal space by using $S_{\alpha\beta}(k)$ and $F_{\alpha\beta}(\mathbf{k}, t)$. I have found that the change in the local order upon mixing is followed by the development of an additional longer length scale, which is revealed by the first sharp diffraction peak in the partial $S_{LiLi}(k)$. Because the changes in local order on mixing are much more pronounced in LiF/KF than in LiCl/KCl, the consequent intermediate-range order is also much more pronounced in the former. Associated with the equilibrium intermediate-range order is a characteristic intermediate-range order dynamics, which is very clear in the Li^+ dynamics, and because of the strong coupling in LiF/KF, it is also manifested in the K^+ dynamics in LiF/KF. This strong coupling thus makes reasonable the fact that b_K also decreases in the mixture as b_{Li}, so that isotherms of type II are found in LiF/KF. Thus, the $S_{\alpha\beta}(k)$ and $F_{\alpha\beta}(\mathbf{k}, t)$ functions shown here provide a more qualitative and quantitative characterization of proposed coupling mechanisms in models for the Chemla effect. For instance, from the range of the observed first sharp diffraction peak in LiF/KF, one estimates $2\pi/k_{FSDP} \approx 5$ Å as the typical spatial extension of this characteristic intermediate-range order, which is quite reasonable in light of $g_{\alpha\beta}(r)$ shown in Figures 2−4. (The first minimum of $g_{LiK}(r)$ in LiF/KF, not shown here, is located at 5.0 Å.)

Intermediate-range order is a fundamental issue in the structure and dynamics of supercooled glass-forming liquids. Here, it has been discussed with the specific aim of revealing structural and dynamical coupling between the ions in the mixtures and its possible relationship to cation internal mobilities and the Chemla effect. However, the presence of such a clear

indication of intermediate-range order in the simple LiF/KF system deserves further simulation work applicable to the wide phenomenology related to this issue. For instance, it has been proposed that the intermediate-range order could be related to vibrational excitations in this spatial range, the so-called boson peak, which is observed in neutron- and light-scattering spectra.[10] It would be interesting to perform further MD simulations of LiF/KF to reveal a detailed picture of extended and localized vibrations and their connection to the presence of intermediate-range order. Finally, it is worth remembering that all of the MD simulations performed in this work have been done with a nonpolarizable pairwise additive potential model. Were a given fluoride anion allowed to be polarizable, it would become polarized in a very asymmetric neighborhood made of disparate cations such as Li^+ and K^+. Most probably, the remarkable mixing effects on local and intermediate-range structures in LiF/KF would become even more pronounced whether or not polarization effects had been included in the simulations, which also deserves future investigations.

Acknowledgment. The computation facilities of the LCCA at the Universidade de São Paulo is acknowledged. I am indebted to FAPESP and CNPq for financial support.

References and Notes

(1) Chemla, M.; Okada, I. *Electrochim. Acta* **1990**, *35*, 1761.
(2) Okada, I. *Electrochemistry* **1999**, *67*, 529.
(3) Okada, I. *J. Mol. Liq.* **1999**, *83*, 5.
(4) Caccamo, C.; Dixon, M. *J. Phys. C* **1980**, *13*, 1887.
(5) Lantelme, F.; Turq, P. *J. Chem. Phys.* **1982**, *77*, 3177.
(6) Ribeiro, M. C. C. *J. Chem. Phys.* **2002**, *117*, 266.
(7) Miyamoto, Y.; Okazaki, S.; Odawara, O.; Okada, I.; Misawa, M.; Fukunaga, T. *Mol. Phys.* **1994**, *82*, 887.
(8) Koura, T.; Matsuura, H.; Okada, I. *J. Mol. Liq.* **1997**, *73*−*74*, 195.
(9) Klemm, A. *Z. Naturforsch., A* **1984**, *39*, 471.
(10) Quitmann, D.; Soltwisch, M. *Philos. Mag. B* **1998**, *77*, 287.
(11) Sangster, M. J. L.; Dixon, M. *Adv. Phys.* **1976**, *25*, 247.
(12) Larsen, B.; Førland, T. *Mol. Phys.* **1973**, *26*, 1521.
(13) Belonoshko, A. B.; Ahuja, R.; Johansson, B. *Phys. Rev. B* **2000**, *61*, 11928.
(14) Lundén, A.; Okada, I. *Z. Naturforsch., A* **1986**, *41*, 1034.
(15) Janz, G. J. *J. Phys. Chem. Ref. Data* **1975**, *4*, 871.
(16) Janz, G. J. *J. Phys. Chem. Ref. Data* **1974**, *3*, 1.
(17) Allen, M. P.; Tildesley, D. J. *Computer Simulation of Liquids*; Clarendon Press: Oxford, U.K., 1987.
(18) Klemm, A. *Z. Naturforsch., A* **1977**, *32*, 927.
(19) Hansen, J. P.; McDonald, I. R. *Theory of Simple Liquids*; Academic Press: London, 1990.
(20) Okada, I.; Okazaki, S.; Horinouchi, H.; Miyamoto, Y. *Mater. Sci. Forum* **1991**, *73*−*75*, 175.
(21) Elliot, S. R. *Physics of Amorphous Materials*; Longman Scientific & Technical: Harlow, U.K., 1990.
(22) Crichton, W. A.; Mezouar, M.; Grande, T.; Stølen, S.; Grzechnik, A. *Nature* **2001**, *414*, 622.
(23) Wilson, M.; Madden, P. A. *Phys. Rev. Lett.* **1998**, *80*, 532.
(24) Massobrio, C.; Pasquarello, A. *J. Chem. Phys.* **2001**, *114*, 7976.
(25) Wilson, M.; Madden, P. A. *Phys. Rev. Lett.* **1994**, *72*, 3033.
(26) Abramo, M. C.; Caccamo, C.; Pizzimenti, G.; Parrinello, M.; Tosi, M. P. *J. Chem. Phys.* **1978**, *68*, 2889.
(27) Iyetomi, H.; Vashishta, P. *Phys. Rev. B* **1993**, *47*, 3063.